HDC-6-85
ICR-Report-121-85-2

COMPOSITION AND ENERGY SPECTRA OF COSMIC RAY NUCLEI ABOVE 500 GeV/NUCLEON FROM JACEE EMULSION CHAMBER EXPERIMENTS

THE JACEE COLLABORATION

COSMIC RAY RESULTS ON ULTRA–RELATIVISTIC NUCLEUS–NUCLEUS INTERACTIONS BY BALLOON EMULSION EXPERIMENT

THE JACEE COLLABORATION

HIGH ENERGY COSMIC RAY OBSERVATORY

Takeshi SAITO

GAMMA RAY AND NEUTRINO DETECTIONS WITH SPACE STATION AND DUMAND

Takashi KITAMURA

ICR Contributions to
Workshop on Cosmic Ray and High Energy Gamma Ray
Experiments for the Space Station Era
Louisiana State University
Baton Rouge, LA
17 – 20 October, 1984

Institute for Cosmic Ray Research
University of Tokyo
Tanashi, Tokyo, Japan

COMPOSITION AND ENERGY SPECTRA OF COSMIC RAY NUCLEI ABOVE 500 GeV/NUCLEON FROM THE JACEE EMULSION CHAMBER EXPERIMENTS*

THE JACEE COLLABORATION+

T. H. Burnett(h), S. Dake(b), M. Fuki(c), J. C. Gregory(g), T. Hayashi(g), R. Holynski(i), J. Iwai(h), W. V. Jones(e), A. Jurak(i), J. J. Lord(h), O. Miyamura(d), H. Oda(b), T. Ogata(a), T. A. Parnell(f), T. Saito(a), T. Tabuki(a), Y. Takahashi(f), T. Tominaga(d), J. Watts(f), B. Wilczynska(i), R. J. Wilkes(h), W. Wolter(i) and B. Wosiek(i)

(a): ICR, University of Tokyo, (b): Kobe University, (c): Okayama University of Science, (d): Osaka University, (e): Louisiana State University, (f): NASA, Marshall Space Flight Center, (g): University of Alabama in Huntsville, (h): University of Washington, (i): Institute of Nuclear Physics in Krakow

The composition and energy spectra of cosmic rays (z = 1 to 26) above 10^{12} eV have been measured with the JACEE emulsion chambers (total exposure: about 200 m^2sr hr).

Each detector compr ised a large area thin calorimeter to measure energies of released gamma-rays in nucleus-nucleus interactions in the target section, and a section for incident nucleus charge determination ($\Delta z < 1$). Basically, the spectrum of ΣE_γ (total gamma-ray energy) for each element has been measured ($\Delta\Sigma E_\gamma$ < 25 %). A primary spectrum was deconvolved using the distribution function of k_γ (partial inelasticity into gamma-rays) and assumed power law for the cosmic ray spectrum. Details of the JACEE emulsion chamber and techniques have been presented in Refs. [1 - 3].

The previous JACEE results indicated no change in spectral indices up to 500 TeV and 50 TeV/nucleon for proton and helium spectra, respectively [2]. Flux values of each group C - O, Ne - S and Fe at 10^{14} eV also indicated no significant evidence for heavy nuclei dominance within the limited statistics [3].

Heavy primary spectra ($z \geq 3$) below 10^{14} eV have been obtained as well. The detection efficiency on ΣE_γ and primary charge for low energy heavy nuclei (ΣE_γ < 10 TeV) have been examined by a Monte Corlo method, in which characteristics of dark spots in X-ray films produced by electromagnetic cascades in the calorimeter is directly incorporated. Nucleus-nucleus interaction models used in the calculation are examined to be consistent with the interaction characteristics observed in the past emulsion and the present JACEE emulsion chambers. Recent results for nucleus-nucleus interactions from the JACEE-3 experiment [4] have given parameters for model construction and also improve the distribution $f(k_\gamma)$ for heavy nuclei.

The figures show preliminary results of energy spectra for groups C - O, Ne - S and Fe above 500 GeV/nucleon under the present limited selection criterion of events. When the analysis is complete soon, 20 to 50 events for each group are expected in the region ΣE_γ > 1 TeV. This data will give the ratios of PRIMARY to PRIMARY and SECONDARY to PRIMARY

above 500 GeV/nucleon, and confirmation for mass composition at 10^{14} eV. These results will then give constraints on model of cosmic ray sources and their distribution, and cosmic ray propagation mechanism through interstellar space.

References

[1] Huggett, R. W. et al., Proc. 17th Intern. Cosmic Ray Conf. (Paris), 8 (1981) 80.

[2] Burnett, T. H. et al., Phys. Rev. Lett., 51 (1983) 1010.

[3] Burnett, T. H. et al., Proc. Intern. Symposium on Cosmic Rays and Particle Physics (Tokyo), (1984).

[4] Parnell, T. A. et al., presented in Quark Matter '84 (Helsinki), (1984). This experiment has given the multiplicity, angular distribution of secondary charged particles, total number of electromagnetic shower particles as a function of energy and non-wounded (spectator) portion of projectile nucleus and fragmentation probability scheme, using about 100 nuclei of iron group ($z \geq 22$) with known energies 20 to 60 GeV/nucleon, as well as the primary spectra ($z = 6$ to 26) above 20 GeV/nucleon. For instrumentation, see Austin, R. W. et al. and Burnett, T. H. et al., Proc. 18th Intern. Cosmic Ray Conf. (Bangalore), 9 (1983) 375, 379.

---

* This work was supported in part by the ICR, the JSPS and the Kashima Foundation in Japan; in part by the DOE, the NASA and the NSF in the USA.

+ Mailing Address: Institute for Cosmic Ray Research, University of Tokyo, Tanashi, Tokyo 188, JAPAN, and Research Institute, University of Alabama in Huntsville, Huntsville, Alabama 35899, USA.

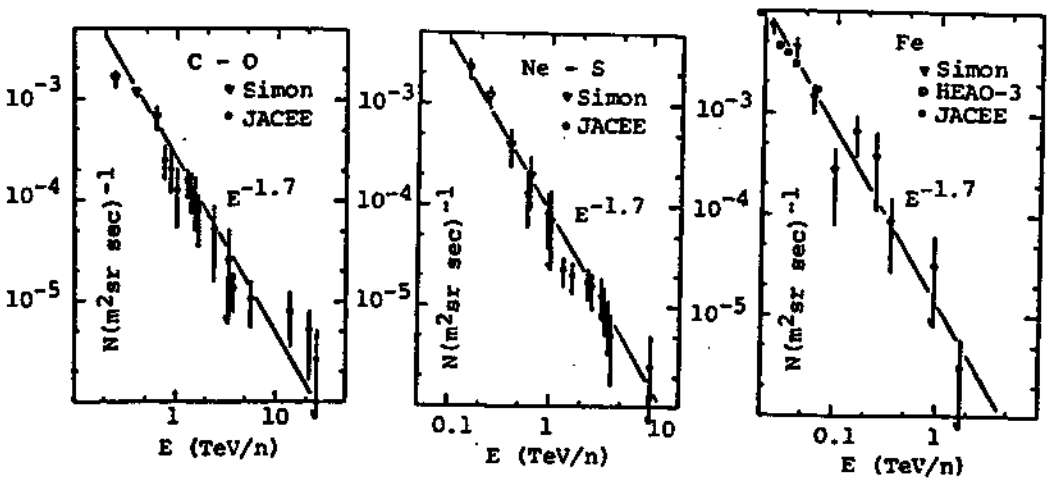

Cosmic Ray Results on Ultra-relativistic Nucleus-Nucleus Interaction by Balloon Emulsion Experiment

JACEE collaboration

T.H.Burnett[h] S.Dake[b] J.H.Derrickson[f] W.Fountain[f] M.Fuki[c] J.C.Gregory[g] T.Hayashi[g] T.Hayashi[b] R.Holynski[i] J.Iwai[a] W.V.Jones[e] A.Jurak[i] J.J.Lord[h] C.A.Meegan[f] O.Miyamura[d] H.Oda[b] T.Ogata[a] T.A.Parnell[f] E.Roberts[f] T.Saito[a] S.Strausz[h] T.Tabuki[a] Y.Takahashi[f] T.Tominaga[d] J.W.Watts[f] B.Wilczynska[i] R.J.Wilkes[h] W.Wolter[i] and B.Wosiek[i]

a.Institute for Cosmic Ray Research, University of Tokyo
b.Physics Department, Kobe University
c.Okayama University of Science
d.Department of Applied Mathemetics, Osaka University
e.Department of Physics and Astronomy, Louisiana State University
f.Marshall Space Flight Center, NASA
g.Department of Chemistry, University of Alabama in Huntsville
h.Department of Physics, University of Washington
i.Institute for Nuclear Physics, Krakow

1. Introduction

Formation and observation of new states of hadronic matter is one of interests in dynamics of quark and gluon system. The expected phases, Quark Gluon Plasma (QGP) and Chiral Symmetric Phase (CSP), would be realized under extreme condition of high temperature and high pressure.[1] High energy cosmic ray nuclei provide unique test ground on this subject. JACEE collaboration is now continuing to sample nucleus-nucleus interactions at high energies(10-100 GeV/A) and super high energies (above TeV/A)[2] in order to find clues of the new phases. In this report, present[3] results obtained from five balloon emulsion experiments are presented.

2. Experimental procedure and data sampling

Apparatus utilized are balloon borne emulsion chambers. Typical structure of the emulsion chamber is shown in Fig.1.[4] Upper part of the chamber is primary charge analyzer module composed of plastic CR39 and low sensitivity emulsion. Below the primary charge analyzer module, target layer consisting of thin emulsion coated on lucite base is set. Middle part of the chamber is spacer region for separation of gamma rays. The bottom is calorimeter module including lead, X-ray film and emulsion. The apparatus enable us to measure charge of primary nucleus and those of nuclear fragments. As for the charged tracks , emission angle and azimuthal angle are determined with high accuracy. The energy and angles of each gamma rays are also measured by cascade shower analysis. Detection threshold of the calorimeter for a photon is 30 GeV. From those imformations we obtain pseudo-rapidity distributions of nuclear fragments, charged track and photon and transverse momentum distribution of photon. Energy of

primary nucleus is estimated mainly by Castagnoli-method and total energy of gamma rays.

A counter-emulsion hybrid system has been used in JACEE-3 flight for sampling cosmic ray nuclei in energy range 20 GeV/A to 60 GeV/A. Main structure of the system is shown in Fig.2. By the use of counter system, energy and position of primary cosmic ray nucleus are measured. In this case, measurement of transverse momentum of photon is not available due to detection threshold of calorimeter.

Up to the last year(83), five balloon flights have been successfully performed as shown in Table 1.

Table 1. JACEE balloon flights

Flight	Date	Place	Altitude	Duration	Area
JACEE-0	5/79	Sanriku	8.0 gr	29.0 hr	0.2 m^2
JACEE-1	9/79	Palestine	3.7 gr	26.5 hr	0.8 m^2
JACEE-2	10/80	Palestine	4.0 gr	29.6 hr	0.8 m^2
JACEE-3	6/82	Greenville	5.0 gr	39.0 hr	0.25 m^2
JACEE-4	9/83	Palestine	4.5 gr	56.0 hr	0.8 m^2

3. Results of nucleus-nucleus interaction in the energy region above TeV/A

In the present stage of analysis, about two hundred non-peripheral events with $\Sigma E_\gamma > 5$ TeV have been observed in the chambers of JACEE-0,1,2,4 (total exposure is roughly 200 $m^2 \cdot str \cdot hr$). Amongs this events sample seven events having multiplicity greater than 400 have been observed as shown in Table 2.

Table 2. High multiplicity events (Nsh 400)

Projectile/Target	E/A	Nsh	N	dNsh/dη(Max)	
Si/Em	4 TeV	1030± 30	>170	180	*
Ca/CHO	120 TeV	760± 30	>300	100	*
Fe/Pb	~2 TeV	1050± 100		240	*
Si/Pb	4 TeV	>700			
Ca/Pb	.5 TeV	680		140	
Fe/Pb	1.5 TeV	500			
Ar/Pb	1 TeV	416	>76 +16 π^0	120	*

* means that energy density is larger than 1 GeV/fm^3

Three of them, Si/Em(4 TeV/A), Ca/CHO(120 TeV/A) and Fe/Pb(1~2 TeV/A) have been already reported. In Fig.3 ,pseudo-rapidity distribution of the Ca/Pb event are presented. The distributions are single bump and their maximum heights are rather high. In the case of the Fe/Pb (1~2 TeV/A) event, it reachs 240. Although several models[6] based on superposition of nucleon-nucleon or quark-quark collision reproduce such high multiplicities in case of head-on collision, high pseudo rapidity density and relatively large value of average transverse momentum in such events lead to large energy densisy exceeding 1 GeV /fm^3 in which superposition can not be justified.

Transverse momentum distribution of gamma rays is obtained from

cascade shower analysis. In the total event sample, there is a group of events having flatter transverse momentum distribution of photon in comparison with that of hadron-hadron or hadron-nucleus collision with similar incident energy. Actual shape of distribution varys event to event and some times two component structure is obtained. In Fig.4 typical examples of the distributions are shown. In the case of CA/CHO (120 TeV/A) event, single exponential shape is observed and average value of transverse momentum of pion (gamma rays are assumed to be decay products of neutral pion) is estimated to be 700 MeV/c which is remarkably larger in comparison with the value,400-500 MeV/c,observed in $\bar{p}$-p collider of CERN. As already mentioned, most of high multiplicity events belong to this group. Origin of such increase of transverse momentum is now question to be solved and is discussed from different view points. Multiple scattering and nuclear enhancement of hard scattering are possible example of conventional explanation. In Fig.4 curve shows a calculation of transverse momentum distribution of multi-chain model in which multiple scattering of nucleons is taken into account. Such effect is small for the distribution in mid rapidity region although it is important in the fragmentation region. The nuclear enhancement of hard collision have been observed in alpha-alpha collision in CERN. Although hard collision is enhanced by factor of product of target and projectile mass number, it seems difficult to push up average value of transverse momentum. This is because soft component in the high multiplicity events is also strongly enhanced as shown in Table 2.

In Fig.5 scatter plot in the plane of average transverse momentum and energy density is shown. The latter quantity is estimated from the observed pseudo-rapidity density in mid rapidity region and average transverse momentum through the Bjorken's formula[5]

$$\epsilon = \frac{3}{2}\sqrt{\overline{p_T^2} + m_\pi^2}\,(dN/d\eta)_{\eta=0} / (c\pi A_{Min}^{2/3})$$

where A_{Min} is $Min(A_{Proj}, A_{Target})$ and c is chosen to be 2 fm^2. In the figure ,nucleus-nucleus events and hadron-nucleus events of which measurement of transverse momentum has been unambiguously done are plotted. In this plot we see that growth of average transverse is apparent for the events having energy density exceeding GeV/fm^3. Such correlation is consistent with the change of equation of state of hadronic matter if average transverse momentum simulates temperature of collision complex[7,10] At present number of high energy density events is small for further analysis although this feature seems to be suggestive. Analysis based on large event sample will be required. Besides the results mentioned above,several notable features are observed. Structured pseudo-rapidity or azimuthal angle distributions in high the high multiplicity events is one of them.[12,13] Pairing of tracks in emission angle is observed in some events.[11] Although these features may have relevance with the expected transition it seems difficult to extract the meaning without prejudice due to

lack of knowledge of nature of the transition.

4. Fe interactions at energies 20 - 60 GeV/A by counter-emulsion hybrid system

In the energy region 20 to 60 GeV/A, events induced by nuclei around Z=26 have been sampled and analized selectively. Interaction in this energy region is considered to be relevant to compressibility and collective flow of nuclear matter. By the use of the hybrid system shown in Fig.2, charge and energy of primary nuclei are selected. In Table 3,number of events, inclusive quantities are presented for the interaction of nuclei(Z=22 -26) with light target(CHO),emulsion and lead plate.

Table 3.

Target	Number of event	$Nsh(\theta<\theta_h)$*	$D(\theta<\theta_h)$	E
CHO	53	17.6 ± 2.6	19	35.2
Emulsion	10	30.6 ± 13.9	44	27.7
Pb	14	46.1 ± 11.1	42	34.3

θ_h is half angle defined by $\tan\theta_h=2m_N/\sqrt{s}$

For CHO interactions, 53 events corresponds to roughly cross-section of 2 barn. It is noted that peripheral interaction with multiplicity less than two is biased. Therefore the obtained value should be understood as an estimate of total inelastic cross-section without very peripheral one. In the table, multiplilicity and dispersion in forward cone are given. This is because tracks in backward hemisphere some times can not be measured due to bad condition of vertex position. (N/D) ratio from the table seems to be twice larger than that of hadron-hadron scattering. This increase of dispersion can be understood as freedom of impact parameter. In Fig.6, scattering plot in plane of multiplicity and incident energy/nucleon is shown. Average values of multiplicity of Fe-CHO interactions are represented by crosses. For the sake of comparison average forward multiplicity of proton-proton collision is presented with suitable multiplication factor. As far as the average multiplicity drastic change of energy dependence is not found. The value of multiplication factor 8.8 is also consistent with average collison number in the Glauber model

$$A A' \sigma_0 / \sigma_{AA'} = 12.$$

As primary interest of nucleus-nucleus interaction is in central collision, high multiplicity events in emulsion and lead targets and central collisions of Fe-CHO events are examined. In Fig.7, pseudo-rapidity distributions of Ti(26 GeV/A)/Em and Ti(41 GeV/A)/Pb are shown. Forward multiplicity of these events are 133 and 134 which are three standard deviation from average value shown in Table 3 and much bigger than values of Multi-Chain model[8] and wounded nucleon model[9] in head-on collision. The maximum height of pseudo-rapidity densities are 90 and 120 ,respectively and are comparable with those of high-multiplicity events above TeV/A region. Although we have no way to estimate energy density and baryon number density in this energy

* Exactly speaking, $N_{sh}(\theta<\theta h)$ is defined as

$$\sum_{\theta_i<\theta_h} |Z_i| - Z_{projectile}.$$

region, these high pseudo rapidity density would be related with formation of dense collision complex.

In order to select central collision in Fe-CHO interactions, tracks emitted in very forward cone are defined as evapolation particles. For this purpose, average value of $\tan\theta$ is calculated for the particles in the region $\theta=0-\theta_f$. Changing θ_f, the average value of $\tan\theta$ is adjusted to that calculated from boosted Goldhaber's formula(evaporation temperature is set to be 10 MeV). In Fig.8, scatter plot in plane of forward multiplicity and total charge carried by evapolation particles in Fe-CHO interactions is presented. Inclusive distribution of the events with total evapolation charge less than 14 is presented presented in Fig.9. The number of such events is 15 and a quarter of total Fe-CHO events. In this case average forward multiplicity is 36 and particle production in mid pseudo-rapidity region is significant. Among these events, one event Fe(55 GeV/A) /CHO has very large multiplicity and dipole type azimuthal distrbution as shown in Fig.10. Although only one event has been found at present, existence of such event may be suggestive for collectiveness of nucleus-nucleus collision in this energy region.

References

1) For example ,E.V.Shuryak, Phys.Report 61C 71 (1980) , H.Satz(ed) Statistical Mechanics of Quark and Hadron ,North Holland (1981).
2) Proceedings of the Quark Matter '83 (ed. by T.Ludlum and H.Wegner) Nucl.Phys. A418 (1984).
3) T.H.Burnett et al. JACEE collaboration, Phys.Rev.Letters 50 2062(1983)
4) T.H.Burnett et al. JACEE collaboration, Phys.Rev.Letters 51 1010(1983).
5) J.D.Bjorken, Phys.Rev. D27 140 (1983).
6) H.Sumiyoshi, Phys.Lett. 131B 241 (1983), A.Capella, C.Pajares and A.V.Ramallo, preprint TH.3700-CERN A.Dar and B.Margolis , McGill University preprint.
7) M.Gyulassy , Nuclear Phys. A418 59c (1984).
8) K.Kinoshita, A.Minaka and H.Sumiyoshi, Z.Phys. C8 205 (1981).
9) A.Bialas,M.Bleszynski and W.Czyz , Nucl.Phys. B111 461 (1976).
10) L.Van hove, Phys.Lett. 118B 138 (1982).
11) P.S.Freier and C.J.Waddington, AIP Conf. Proc. 49 87 (1978).
12) L.Van Hove, CERN preprint TH3592-CERN.
13) F.Takagi, Phys.Rev.Lett. 53 427 (1984).

#Address for correspondence
Institute for Cosmic Ray Research, University of Tokyo
188 Tanashi, Tokyo, Japan
Department of Physics and Astronomy, Louisiana State University
Baton Rouge, LA 70803 USA

$This work is supported by ICR,JSPS,Kashima Foundation in Japan and DOE,NASA and NSF in United State.

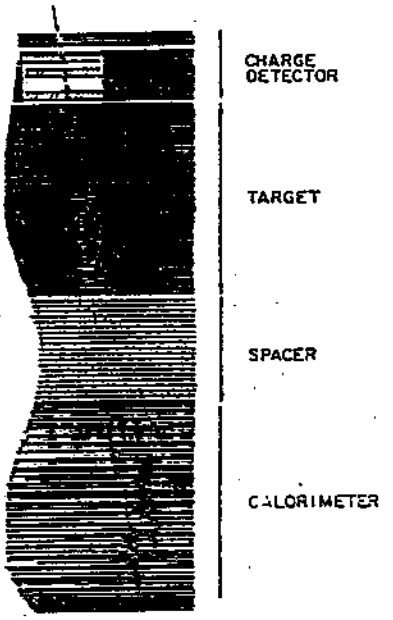

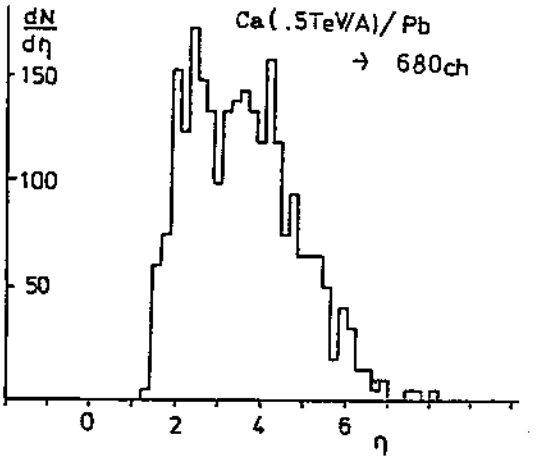

Fig. 3

Fig. 1

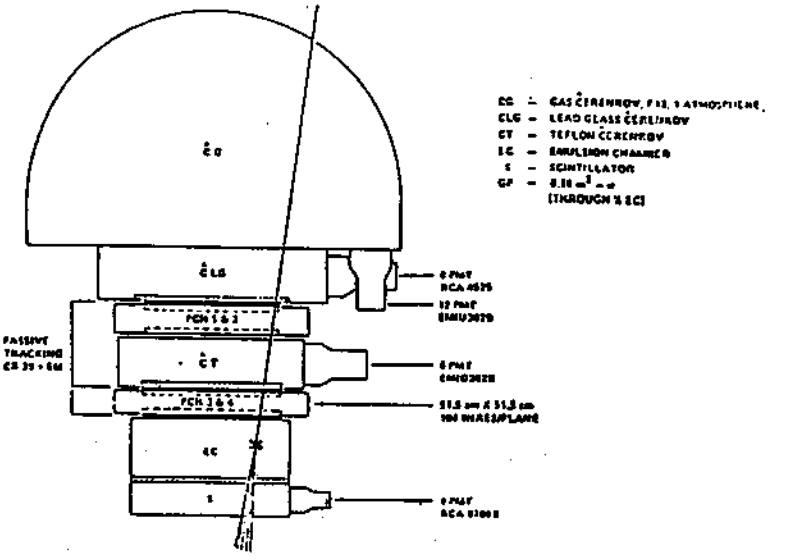

Fig. 2. JACEE-3 hybrid system

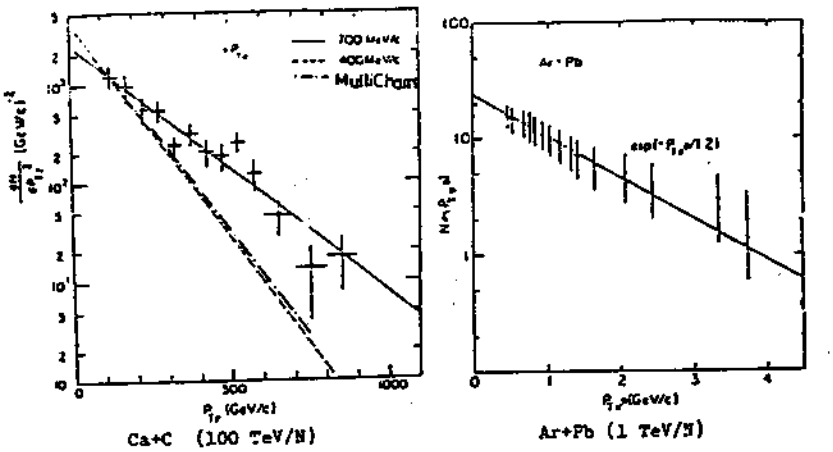

Fig. 4 Transverse momentum distributions

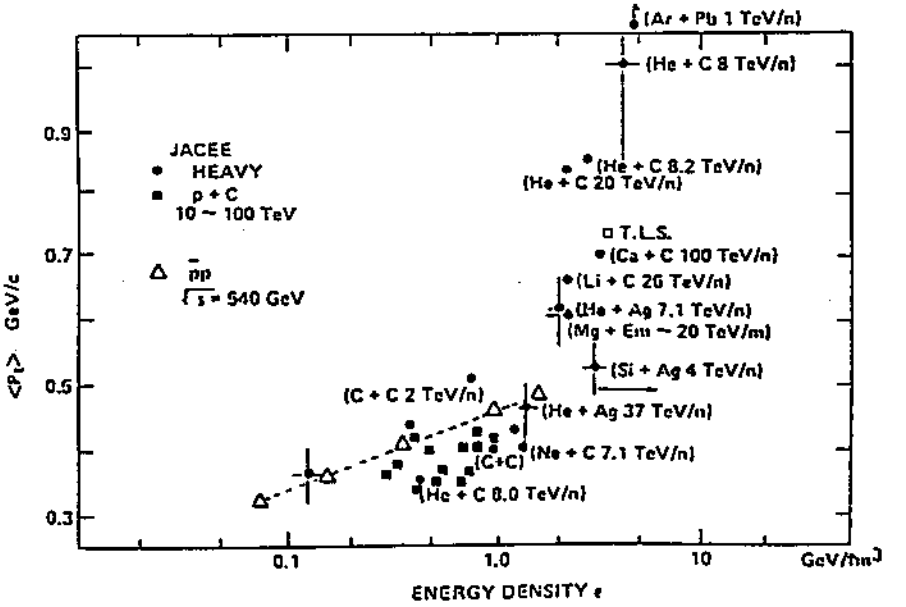

Fig.5 Transverse momentum-energy density correlation

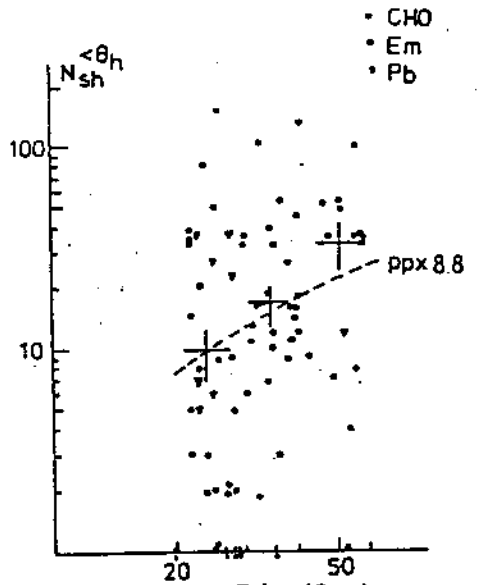

Fig. 6

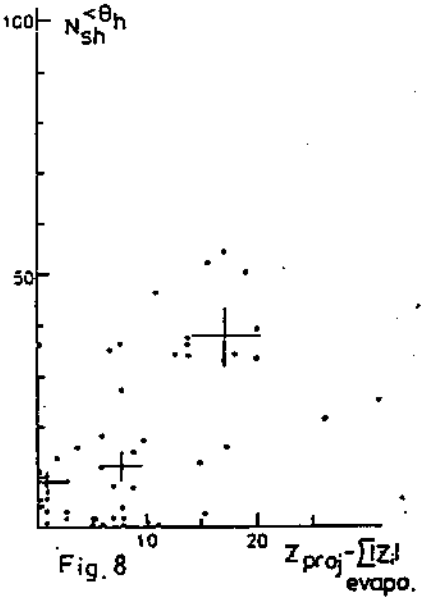

Fig. 8

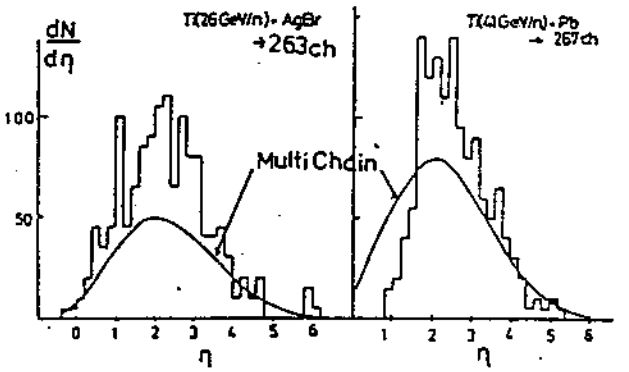

Fig. 7

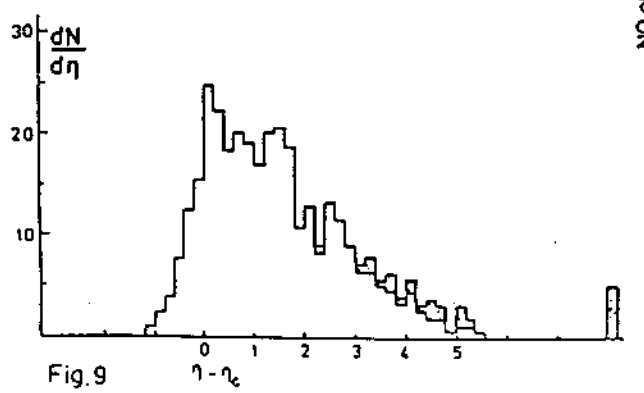

Fig. 9

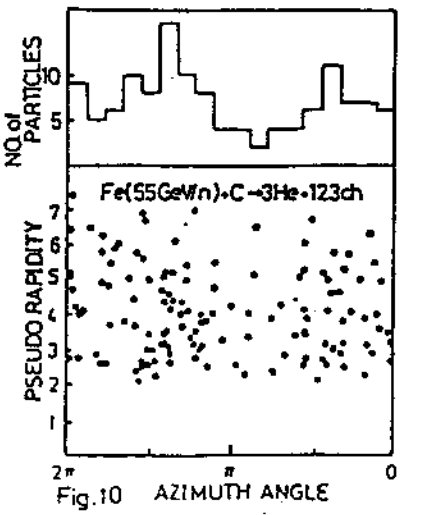

Fig. 10

HIGH ENERGY COSMIC RAY OBSERVATORY

Takeshi SAITO
Institute for Cosmic Ray Research
University of Tokyo
Tanashi, Tokyo, Japan

ABSTRACT

Construction of space station facilities, High Energy Cosmic Ray Observatory is proposed to study the high energy gamma rays, nuclear composition and spectra, and nucleus interactions. Objectives, experimental consideration, and plans for technical and calibration studies are presented.

1. Introduction

This is a proposal to construct the observatory in space by the name of HECRO, High Energy Cosmic Ray Observatory. The HECRO is a simple thin electromagnetic transition calorimeter which is designed to study the gamma rays at energies of 1 to 1000 GeV, nuclear composition and spectra at the bend, 10^{15} to 10^{16} eV/nucleus, and nucleus interactions at energy regions greater than 100 TeV. Basic idea of HECRO design is the same as the JACEE passive detector but with counter system and without nuclear emulsions. Observation is expected in the 1990's. It is necessary to improve the present techniques as well as to develope new detectors in order to complete the HECRO project in coming years to the 1990's. Moreover, an education of the rising generation of scientists is also seriously important for these p ses.

2. Objectives

1) High Energy Gamma Ray Observation

Interests and objectives in the high energy gamma ray astronomy shown in Table-1 are our common understanding and so it may be not necessary to mention it much. The detection of at least 4 classes of gamma ray sources with remarkably different characteristics is especially important, pulsar (2CG184+05, 2CG263-02), closed binary system (CygX-3), Moleculardlouds (2CG253+16;ρOph) and Active galactic Nuclei (3C273, Cen A).

(1) Although detection of many pulsars has been claimed, there have been only two pulsars, PSR531 (Crab) and 0833 (Vel), which have been identified firmly on the basis of the periodicity of gamma rays. Continued observations of these familiar sources is required at higher energy region.

(2) The binary system, CygX-3, was insisted to be detected at energy of around 40 MeV by it s periodical variation of 4.8 hr. However no confirmation is given in the COS-B experiment. There have been extensive studies for CygX-3 over a wide range of frequencies from the radio to the ultra-high energy of around 10^{15} eV. The gamma rays at the ultra-high energy regions were claimed to be detected with the ground-based Cherenkov detectors and air shower detector array. However, it is important to detect this presence of extremely variable high energy out put at the higher energy regions with direct method because the detection at energy around 100 MeV is still uncertain.

(3) Among 25 point sources observed by COS-B experiment, only four sources have been identified, Crab, Vela, 3C273 and ρOph. Out of 21 unidentified sources, 20 sources are closely aligned with the galactic disc and properties of these unidentified gamma ray sources have been discussed. Observation at higher energy regions is necessary together with identification with known astrophysical objects.

(4) Recent gamma ray observation of active galaxies provides important understanding of the activities in their nuclei, Radio galaxies, Seyfert galaxies and quasars. The lumious out put of the active galaxies are 10^{42} to 10^{48} ergs sec^{-1} which corresponds to 10^{8} to 10^{14} times the solar luminosity. In order to explain these compact and supermassive objects, various models have been proposed, rotating magnetized plasma (spinar or magnetoid) or supermassive black holes accreting matter.
For Example, one theory proposed recently by Kafatos (1980) attributes the output within the active nucleus to Penrose collision process in the ergoshere of a massive Kerr black holes. They attribute the observed sharp break in the MeV region of the NGC4151 to the Penrose Compton scattering. The absence of a MeV break in the spectra of Cen A and 3C273 is insisted to be explained by the Penrose pair production. If true, a sharp break in the GeV region, around 2 GeV, is expected in the spectra of Cen A and 3C273. The extraporated spectra of 3C273 are shown in Figure 1 for two cases with and without the existence of the break. This model is easily checked from the observation at energy around 10 GeV with collection factor of 100 m^2 hr. as shown by cross area in Figure 1.

TABLE 1

OBJECTIVES OF GAMMA RAY OBSERVATION

SOURCE	COMMENTS
1. PULSAR Crab,Vela	Continued Observation High Energy Spectrum
2. BINARY SYSTEM SygX-3	Nc Confirmation in COS-B Time Variability
3. COS-B 25 Point Sources	Identification. High Energy Spectrum
4. RADIO GALAXIES QUASARS Cen A, 3C273 NGC 4151	Spectral Break(Penrose PP) Time Variability
5. NEW SOURCE SURVEY	
6. GAMMA RAY BURSTS	
7. GAMMA RAY/NEUTRINO	Discrimination Black holes/Spinars

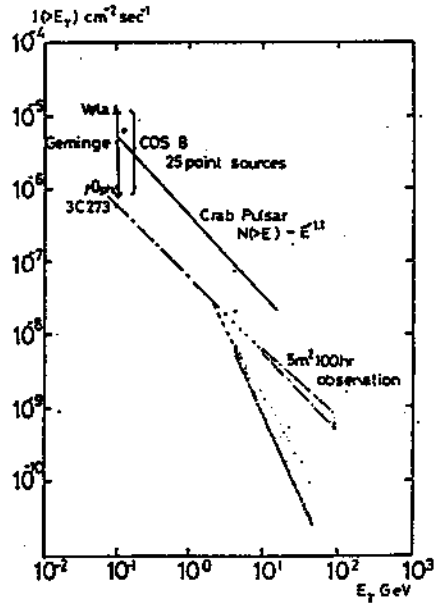

Figure 1.
High Energy Gamma Ray Spectra

(5) A comparison of gamma ray observations with neutrino observation gives the understanding of the nature of active galaxies, especially a discrimination between massive balck hole model and spinar model for active galactic nuclei. The DUMAND proposes to provide the neutrino spectrum at energies greater than 1 TeV.
A combination of HECRO and DUMAND with timing is crucial important for this study.

In order to observe the gamma rays over many decades of energies, different experimental techniques have to be applied. Generally, the scintillator and solid state detectors have been used from energy of 100 KeV to about 20 MeV. Above this energy where most active area of gamma ray observations, the spark chambers are mainly used (SAS-2 and COS-B). As the energy of gamma rays increases, the opening angle of pairs decreases and it becomes increasingly difficult to identify the gamma rays. So the track imaging method such as spark chamber is limited to energies up to several GeV. Moreover, an instrument with a large sensitive area is necessary to observe the gamma ray spectrum beyond several GeV with reasonable statistical accuracy. The HECRO calorimeter system is designed to enter into this energy region with angular resolution of 0.05 degree.

2) High Energy Nuclear Composition and Spectra

Observation of elemental composition and spectra provides the basic information for understanding the acceleration mechanism, confinements and propagations of cosmic ray particles. The energy spectra had been well measured up to energies around 1 TeV for proton, a few hundred GeV/nucleon for He nuclei and about 100 GeV/nucleon for heavier nuclei. As shown in Figure 2, recently, JACEE group (Hayashi et al. 1984) extended the energy range by more than one order and indicates that the ralative abundances and spectra of cosmic ray source nuclei at energy of 10^{14} eV/nucleus does not show any remarkable deviation from the low energy composition, although the statistical accuracy is still limited. The elemental composition of cosmic ray source nuclei is entirely unknown at energies greater than 10^{14} eV/Nucleus. There have been attempts to deduce the composition at energies greater than 10^{15} eV/nucleus from indirect measurements at a deep atmosphere. They insist that the composition becomes enriched in iron nuclei. However, air shower observations have not led to convincing results and direct measurements must solve the composition problems finally.

There have been many speculations for the compostion and spectra at these high energies. For example, assuming the supernova shock acceleration, the spectra will break at these high energies from the reasons that the scattering length increases with energy and becomes compareble to the radius of the shock curvature, and that the acceleration time increases with energy and becomes comparable to the escape time at these high energies. However, direct measurements at energies around 10^{15}/ ncleus are crucial to decide which model for cosmic ray acceleration and containments is favourable. In order to measure the cosmic rays

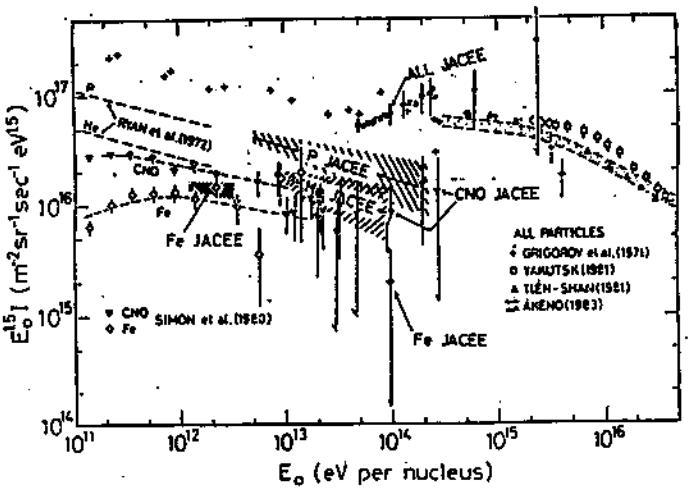

Figure 2.
JACEE result in the composition study.
(JACEE; Hayashi et al. 1984)

at these high energies with reasonable statistical accuracy, it is necessary to make experiments with an instrument of a large geometry factor of at least a few m^2 and with a long exposure time of a year or more. Figure 3 shows the relation between the collecting factor and observable energy ranges. As shown by the broken curve in the figure 3, annual balloon experiments such as the present JACEE scale is limited to the maximum energy of 3 X 10^{14} ev/nucleus even if we continue the balloon flights for more ten years. The LASSEE proposed by Parnell et al.(1984) is planning to open the door of the bending with Large Area Space Shuttle Emulsion Experiment (LASSEE). However, passive detector is limited to exposure time of at most 3 months due to high radiation background. The maximum energy which the passive detector could be applied is around 10^{15} eV/nucleus. The HECRO region is shown in the figure 3. The HECRO is unique measure in the regions of 10^{15} to 10^{16} eV/nucleus.

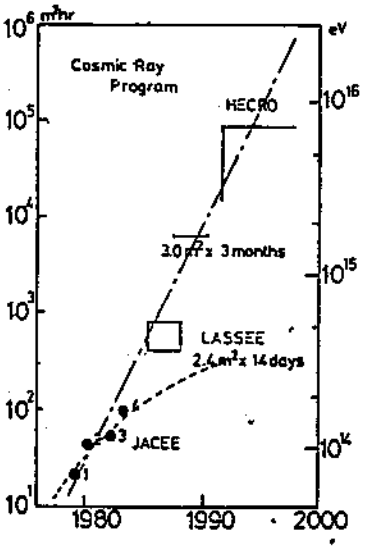

Figure 3.

3) High Energy and High Particle Densities

There have been many arguments about the phase transition from nuclear matter to quark-gluon plasma which is expected to be observed in the high energy nucleus-nucleus collisions. I would like to strongly emphasize that cosmic ray heavy ions are unique facilities to study physics of high energy and high particle densities at present as well as in future. As shown in Figure 4, the planned heavy ion collider will reach to energy regions of 1 TeV/nucleon in the middle of the 1990's. This energy region is exactly focussing now by JACEE. The JACEE results in the nucleus-nucleus interaction study are summarized as follows although statistics is still limited at present.

(1) The productions of events with extremely high multiplicities, more than 1000 and with high rapidity densities of a few hundred are not rare.

(2) The high energy density events with more than 2 GeV/fm^3 are obseved with high production rate around or above some energy. The transverse momentum increses with energy density as shown in Figure 5. The particle with high transverse momentum seem to be produced at the central regions.

(3) The fluctuations in the rapidity distributions seem to be more predominant in comparison with statistical fluctuation.

(3) Copious direct pair production appears in the high energy density events.

However, these results still remain to be

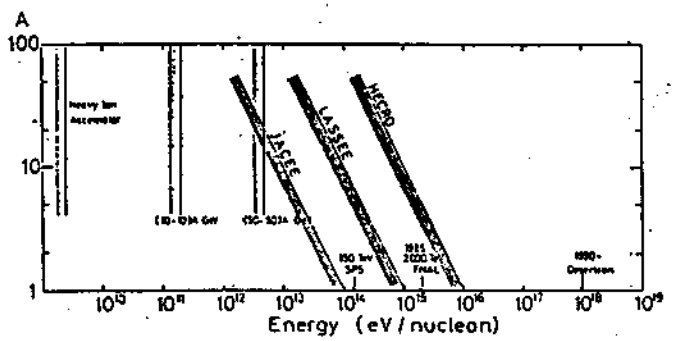

Figure 4.

qualitative. In order to confirm the results, it is necessary to organize more precise experiments with improved instrumentations and methods together with improved statistics. Especially, the measurements of cross section of pair productions and particle identification of the pairs are required. The second phase of cosmic ray heavy ion experiment has to focus to get the detailed nature of high energy density events with balloon or space shuttle experiment like LASSEE.

On the other hand, the so called "anomalies" in the indirect cosmic ray experiments at a deep atmosphere appear above a threshold of about 100 TeV. These anomaly events have not been observed in the proton-antiproton interactions at 150 TeV. The relation of these anomaly events with the high energy density events in JACEE is not certain at present. It is most interested whether high energy heavy ion physics is totally different from physics in the hadron-hadron collisions or not, and moreover whether the temperature (transeverse momentum) increases further with increase of energy density or reachs to constant as shown by broken curve in Figure 5. The HECRO concerns to study these regions. In the direct experiment at energies of 100 to 1000 TeV, it is difficult to separate individual paticle produced from heavy nucleus interactions. So energy flow per some unit volume will be measured in HECRO experiments with thermoluminecent sheet detector.

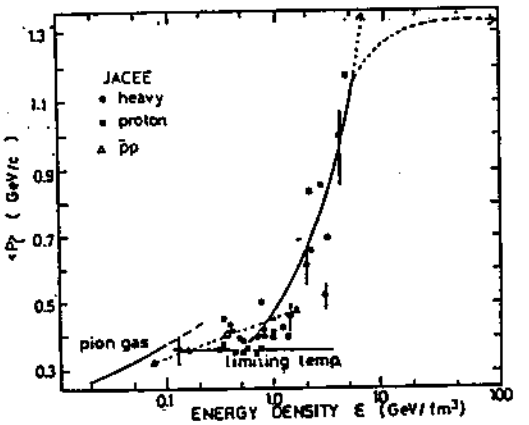

Figure 5.
JACEE result in the interaction study.
(JACEE; Miyamura et al. 1984)

3. Experimental Consideration

1) Limitation of The Present Active and Passive Detectors

There are several techniques to determine the energy of cosmic ray particles. It is possible to measure the energy of cosmic rays with gas Cherenkov detectors at energy up to several hundred GeV/nucleon. The transition radiation detector is useful at energy range greater than several hundred GeV/nucleon but the transition radiation will saturate at energy around several TeV/nucleon. The use of calorimeter is unique method at present to meausre the cosmic rays at energies greater than about 10 TeV/nucleon. However, the calorimeter, generally, has to be several interaction length deep and becomes naturally very heavy, several tons per m^2. An instrument with a geometrical factor of several m^2 is required to observe the composition of cosmic rays at energy above 10 TeV/nucleon with sufficient statistics, assuming one year or more exposure.

JACEE have employed a thin electromagnetic transition calorimeter which can measure the development of electromagnetic cascades of decay products of neutral meson originated from nuclear interactions. It is possible to measure the sum of energies of the electromagnetic components, ΣE_γ, with resolution of 20-30 %. The uncertainties of inelasticities and impact parameters in nucleus-nucleus interactions lead to uncertainty of the absolute flux value in the primary spectra. However, this problem is not so serious because we already know the absolute flux values at lower energy side with passive detectors and hybrid detectors.

The cascade transition type calorimeter makes possible a larger collecting area, 1 m^2 per 1000 Kg. For example, JACEE has reached to the energy region of 10^{14}/nucleus for heavier nuclei through only 4 balloon flights. However, JACEE type passive detector is not applicable to long exposure experiments on board space station because of high radiation background.

The low energy particle background were measured using a small emulsion stacks at several shuttle orbits. One example (STS-6, 300 km height and 28.5°inclination) is shown in Figure 6. On the other hand, the background in the nuclear emulsion and X-ray films exposed for one year at mountain altitude (Mt. Norikura in Japan) was measured to be 7.6 X 10^5 particles per cm^2 and D=0.1 for photometric darkness. This number corresponds to energy of 1 TeV for electromagnetic cascades in D_{max} measurement with 200 micronϕ slit. As shown in Figure 8, photometric darkness in the X-ray films saturates at D=5. If we plan to use the X-ray films as cascade detector with remaining dynamic range of one order, the limit of accepted background is about 4 X 10^6 particles/cm^2. The flux of low energy particle background at shuttle orbit of 300 Km and 28.5°inclination is 5 X 10^5 particles/cm^2 for 5 days under the absorption materials of about several g/cm^2 as shown in Figure 6. So limit of exposure time of JACEE type passive detector is estimated to be 40 days at the same orbit of STS-6. In actual case, we can extend the dynamic range of X-ray films further by factor 5 because we can measure the darkness outside of the saturated core of cascade. Moreover, as we must use the passive detector with lower sensitivities, limit of exposure time will increase by factor 2.

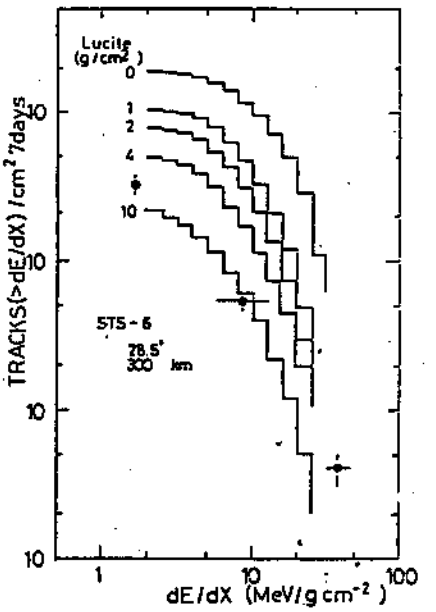

Figure 6.
Background particles in STS-6

2) HECRO System

Schematic view and composition of HECRO are shown in Figure 7 and Table 2. Basic idea of HECRO design is totally the same as JACEE type emulsion chamber but with counter system and without nuclear emulsion. The total thickness of calorimeter is about 15 radiation lengths deep. The developments of electromagnetic cascades are measured at 13 points of different radiation lengths with the proportional and pulse ionization counters. The proprtional counter is applied to energy range of 1-1000 GeV for gamma rays

TABLE 2

DETECTOR COMPOSITION OF HECRO

MEASUREMENTS	DETECTORS	REMARKS
Discrimination of charged/neutral	Scintillator	
Primary Charge Measurement	Cherenkov Detector	$\Delta Z \leq 0.4$ Backscatter prob
Position Measurement	Drift Chamber or Resistive Cathode PR	$\Delta x < 1$ mm Another option
dE/dX for Low Energy Deposite	Proportional Counter	1-1000 GeV
dE/dX for High Energy Deposite	Pulse Ionization Counter	100-1000 TeV
Energy Flow Measurement	Thermoluminecent Sheet	Δx=50 micron E_γ> 20 TeV

and the pulse ionization counter is applied to energy range above 10^5 GeV. The counters are a simple arries of Al tubes of 20 X 20 mm^2 cross section. As gas is enclosed in the tube itself, a container for the gas counter is not necessary. The drift chamber is made by Al tube array method and is planned to measure the trajectory of particles within accuracy of a few 100 micron meter which corresponds to angular resolution of 0.05 deg. The gas counter made of Al tube arraies with 1.5 m X 1.5 m effective area has been constructed for balloon flight experiments. The HECRO is easily assembled from each isolated detector in the field. The total wight of unit HECRO is designed to be about 1000 Kg.

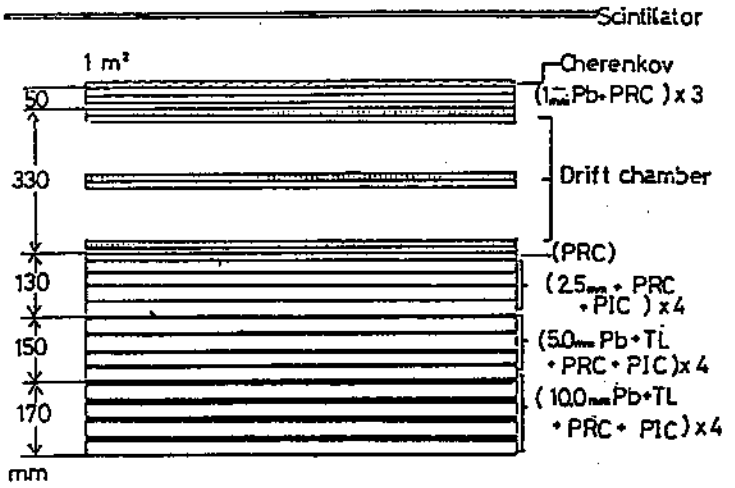

Figure 7.
One unit of HECRO system (1 m^2, 1000 Kg)

3) Thermoluminecent Sheet Detector (TL sheet), Unique Passive Detector in The Long Duration Exposure Experiment

As primary energy increases, it becomes difficult to separete an individual secondary particle due to collimations of the particles from the nucleus-nucleus collisions. The energy flow per some unit volume is measured at such a high energies. However, the traditional passive detector are not applicable because of the saturation of the detectors. The thermoluminescent sheet detector is unique measure in such a high energy study in space, because of the characteristics of TL sheet detector described below.

(1) The detection threshold energy for electromagnetic cascade is around 1 TeV.

(2) The dynamic range covers for 7 orders as shown in Figure 8.

(3) The position resolution for cascade is within 50 micron meter.

(4) Thermal fading effects on the latent TL signal is within 5 % for 6 months under room temperature. Even if we use TL sheet under the temperature of 60°C, the TL signal are reduced to 80 % for first 3 days

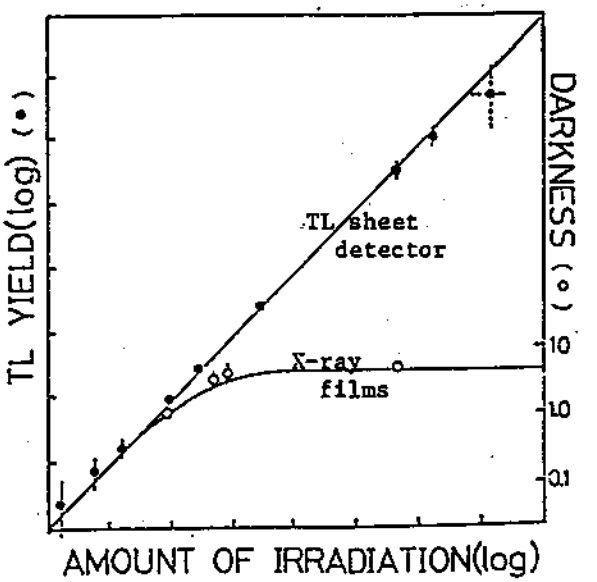

Figure 8.
Dynamic ranges of TL detector and X-ray films (Okamoto et al. 1984)

and stay constant for several months. The dynamic ranges of TL sheet detector is shown in Figure 8 together with that of N type X-ray films for comparison.

Figure 9 shows the increaes of chemical fog density in the nuclear emulsion, keeping it in constant temperature. So temperature control is important in use of the X-ray films and nuclear emulsion. There have been not observed such a problem in the TL sheet detector. The TL sheet detector is also used for cascade detector in ultra high energy regions.

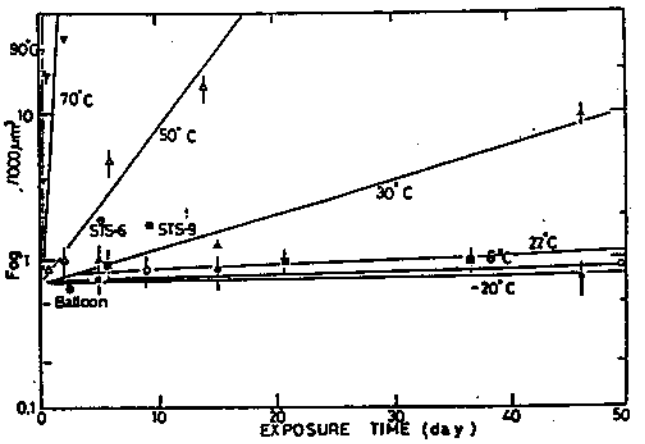

Figure 9.
Relation between fog density and storage time at constant temperature

4. Discussion

We have time more than 5 years before the observation on space station which is expected in the middle of 1990's. It is necessary to make continued efforts in new instrument developments as well as in improvement of the present detectors in coming years to 1990's. The detector compositions of HECRO shown in Figure 7 and Table 2 are one proposal at the beginning stage and especially the position detector and dE/dX detector should be studied.

(1) Prototype of HECRO is planned to construct in Japan. Engineering balloon flight should be done in near future for original design study.

(2) It is necessary for HECRO to know the inelasticities in the nucleus-nucleus interactions. This study should be performed with passive detectors. LASSEE plans to use the instrument composed of Pb plates and photosensitive detectors without taget section. The LASSEE project is most important not only for LASSEE physics but also technical and calibration study for HECRO.

(3) Engineering balloon and/or shuttle flight is also necessary with an unit HECRO system, 1 m^2 and 1000 Kg, for all around enginerring test.

5. Conclusion

吳	越	同	舟	(Chinese story in B.C.~500)
WU	YUN	TONG	ZOU	(Chinese pronunciation)
GO	ETU	DOU	SHU	(Japanese ")

6. References

M.Kafetos, 1980, Ap. J. 236 99.
JACEE, 1984, Presented by T.Hayashi in this work shop.
JACEE, 1984, Presented by O.Miyamura in this work shop.
LASSEE, 1984, Presented by T.Parnell in this work shop.
K.Okamoto et al., 1984, NIM, tobe published.
Chinese story, B.C.~500, One meaning is to cooperate with enemies/rivals each other for thier common objectives.

GAMMA RAY AND NEUTRINO DETECTIONS WITH SPACE STATION AND DUMAND

T. KITAMURA

Institute for Cosmic Ray Research,
University of Tokyo.

ABSTRACT

A measurement with the proposed large calorimeter in the space station can give the flux of gamma-rays with energy greater than 1 GeV, and a measurement by the DUMAND detector can similarly yield the neutrino flux with energy larger than 1 TeV. From these measurements, we can discriminate between models of magnetoids or massive black holes for Active Galactic Nuclei following to Berezinsky et al and Shapiro et al. Also, utilizing both measurements can give the thickness of dense matter surrounding the neutrino source.

§1. Recent observations with X-ray and γ-ray telescopes indicate that many active galactic nuclei (AGN) are X-ray sources and some of them are possible γ-ray sources. They seem to favour supermassive objects as the power sources.[1] These compact, supermassive objects could be: (i) magnetized, rotating plasma masses, e.g., of the spinor or magnetoid type; or else (ii) massive black holes accreting matter. Berezinsky and Ginzburg [2] suggest that a structueless magnetoid and a black hole surrounded by a dense shell of gas or a gas of X-ray photons can be convincingly distinguished by measuring the ratio of neutrino ($E_\nu \gtrsim 1$ TeV) to gamma-ray ($E_\gamma \gtrsim 70$ MeV) fluxes. According to them, the flux of gamma-rays with $E_\gamma \gtrsim 70$ MeV, which accompanies the neutrino flux $E_{\nu_\mu}(>E)$ in the case of a

small depth of matter $x < x_{rad} \approx 60\ gcm^{-2}$, is

$$F_{\gamma,acc} = \lambda(\gamma)\, E^{\gamma}\, F_{\nu_\mu}(>E) \qquad (1)$$

where the neutrino flux $E_{\nu_\mu}(>E)$ is the number of $\nu_\mu+\bar{\nu}_\mu$- neutrinos with energy greater than E emitted by a source per second, and $F_{\gamma,acc}$ is the flux of gamma-quanta with energy $E_\gamma \gtrsim 70$ MeV generated by π° - decays.

Also

$$\lambda(\gamma) = \frac{2\gamma \cdot \sigma_{eff}(\gamma)}{\varepsilon_\nu \cdot \sigma_{in}}$$

$\varepsilon_\nu = \frac{F_\nu(E)}{F_p(E)}$ is neutrino emissivirity coefficients,

and

$$\sigma_{eff} = \int (E+1)^{-\gamma+1} \cdot \sigma_{\pi^\circ}(E)\, dE,$$

Here $\sigma_{\pi^\circ}(E)$ is product of cross section of π°- production and π° multiplicity. σ_{in} is inelastic pp cross section.

Equation (1) was obtained under the assumption that the high energy protons, which produce both neutrinos and gamma-rays, have a power-law differential energy spectrum

$$F_p(E)\, dE = A(E+1)^{-\gamma+1} dE,$$

where E is the proton kinetic energy given in GeV.

The value of λ (λ) are given in Table 1.

Table 1.

γ	1.2	1.4	1.6	1.8	2.0
$\lambda(\gamma)$	5.9	8.3	12.2	17.2	23.8

Since gamma-rays can also be produced by electrons, the gamma-flux in a magnetoid model must obey the inequality

$$F_\gamma\ (\gtrsim 70\ \text{MeV}) > F_{\gamma,acc} = \lambda(\gamma)\, E^{\gamma}\, F_{\nu_\mu}(>E) \qquad (2)$$

If the observed gamma-ray flux with $E_\gamma \gtrsim 70$ MeV does not obey the inequality (2), it is concluded that a gamma-ray flux lower than this predicted value would contradict the model of a structureless magnetoid and support the model of a compact ($\gamma < 10^{15}$cm) cosmic-ray source covered by a gas shell with $x > x_{rad}$ or surrounded by a dense gas of X-ray photons.

§2. The point source sensitivity of DUMAND (the Deep Undersea Muon and Neutrino Detector) can be expressed in terms of the minimum detectable flux (MDF)[3]. The value is about 2×10^{-10} cm^{-2} s^{-1} above 1 TeV when the experimental threshold is set at 1 TeV. Then, if the background "noise" N is large, the MDF is that flux which gives a 4.5σ effect, i.e., $(N-S)/\sqrt{N} = 4.5$. If the noise is small ($\lesssim$1 event per year), the MDF is calculated to be that yields 10 events per year.

When getting a neutrino flux and the spectral index generated from any of AGN as a value of $(2 \times 10^{-10}) \cdot n$ cm^{-2} s^{-1} and a value of γ with operations of DUMAND, we can estimate the value of $F_{\gamma,\ acc}$ $(>E_\gamma)$ using F_{ν_μ} (>1 TeV) = $(2 \times 10^{-10}) \cdot n$ cm^{-2} s^{-1} and the γ-value by using the eg.(1). The predicted values of $F_{\gamma,\ acc}$ are given in Table 2. for various given values of γ.

In this workshop, Saito[4] proposed a construction of the big calorimeter which include the number of m of an unit one with an area of (100 cm x 100 cm), being possible to measure cascade showers in the energy range of 1 GeV to 100 GeV, at the space station. By using the calorimeter, it is easily possible to measure the gamma-ray spectrum with energies of > 1 GeV and its spectral index γ' in a limited operating time. If all the measured gamma-flux is associated with the neutrino flux to be measured by DUMAND, the spectral index of γ' should equal to γ[5]. If the Penrose pair production (ppp) is important[6], it has a contribution to the measured gamma spectrum up to energy as high as $\sim 4m_pc^2$. In that case the measured value of gamma-flux with energy >10 GeV will be used.

Table 2. The predicted values of $F_{\gamma,\,acc}$ ($>E_\gamma$) at various given values of $\gamma' \simeq \gamma$.

γ	$F_{\gamma,acc}$(>70MeV) $cm^{-2}s^{-1}$	$F_{\gamma,acc}$(>1GeV) $cm^{-2}s^{-1}$	$F_{\gamma,acc}$(>10GeV) $cm^{-2}s^{-1}$	$F_{\gamma,acc}$(>100GeV) $cm^{-2}s^{-1}$
1.2	$(4.70 \times 10^{-6})n$	$(1.9 \times 10^{-7})n$	$(1.2 \times 10^{-8})n$	$(7.7 \times 10^{-10})n$
1.4	$(2.6 \times 10^{-5})n$	$(6.4 \times 10^{-7})n$	$(2.5 \times 10^{-8})n$	$(1.0 \times 10^{-9})n$
1.6	$(1.5 \times 10^{-4})n$	$(2.2 \times 10^{-6})n$	$(5.5 \times 10^{-8})n$	$(1.4 \times 10^{-9})n$
1.8	$(8.6 \times 10^{-4})n$	$(7.2 \times 10^{-6})n$	$(1.1 \times 10^{-7})n$	$(1.8 \times 10^{-9})n$
2.0	$(4.8 \times 10^{-3})n$	$(2.3 \times 10^{-5})n$	$(2.3 \times 10^{-7})n$	$(2.3 \times 10^{-9})n$

By using the measured gamma-flux F_γ(>1 GeV) or F_γ(>10 GeV, >100 GeV), we can compare the predicted values of $F_{\gamma,\,acc}$ shown in Table 2. and decide whether $F_\gamma(>E_\gamma) > F_{\gamma,\,acc}\,(>E_\gamma)$ or not. Thus, it is certainly solved the problem of the model of massive black holes or magnetoids (Spinars) for the nature of the cores in guasars and active galctic nuclei.

Let us estimate the flux of background diffuse gamma rays because it might prevent the measurement of $F_\gamma(>E_\gamma)$ with the calorimeter. The diffuse gamma-ray spectrum[7] may be given by a form of $2 \times 10^{-2}E^{-2}$ dE $cm^{-2}s^{-1}sr^{-1}MeV^{-1}$ above 10 MeV. The integral value at several energies of gamma-rays are tabulated in the second column of Table 3.

Table 3. Integral flux of the diffuse gamma rays and its background flux with the calorimeter measurements in the case of angular resolution of (1° x 1°).

E_γ(GeV)	$cm^{-2}s^{-1}sr^{-1}$	$cm^{-2}s^{-1}$ (1° x 1°)
>0.7	2.9×10^{-4}	8.7×10^{-8}
>1.0	2×10^{-5}	6×10^{-9}
>10	2×10^{-6}	6×10^{-10}
>100	2×10^{-7}	6×10^{-11}

Even when setting an angular resolution of 1° x 1° of the calorimeter, the background flux is very low compared with the values of $F_{\gamma,\ acc}$ in Table 2 for a case of $n \gtrsim 1$. The angular resolution with 0.1° x 0.1° is not so difficult. Accordingly, the contribution of diffuse gamma-rays is quite negligible.

§3. The emission of neutrinos and photons from a point source of very high energy proton surrounded by dense matter has been calculated by Stenger[8] and Lee and Bludman[9]. The behavour may correspond to the Crab and Vela pulsars and Cugnus X-3 etc. They have calculated the values of neutrino yield to gamma-ray yield and have shown that the ratio for $\varepsilon_\nu/\varepsilon_\gamma$ ($\varepsilon_i = \frac{F_i(E,Z)}{F_p(E,)}$, $i = \gamma,\ \nu_\mu+\bar{\nu}_\mu$) is independent of energy band E.

The measurement of the calorimeter in the space station can give the values of F_γ (>10 GeV ∿ 100 GeV) and its spectral index γ', and the measurement of DUMAND the values of F_γ (>0.5 TeV ∿ 10 TeV) and its spectral index γ. From the latter F_ν (>10 GeV ∿ 100 GeV) measurement, we can evaluate the value of F_ν (>10 GeV ∿ 100 GeV) because the spectral index of neutrino generated from the source is valid for very wide range of neutrino energy according to their calculations. If the index $\gamma = \gamma'$, the calculated model is valid. Then we can get

$$\frac{\varepsilon_\nu}{\varepsilon_\gamma} = \frac{F_\nu\ (>10\ \text{GeV} \sim 100\ \text{GeV})}{F_\gamma\ (>10\ \text{GeV} \sim 100\ \text{GeV})}$$

and decide the thickness of matter surrounding the source from their calculation, because their calculations have shown values of $\varepsilon_\nu/\varepsilon_\gamma$ as a function thickness of matter at a given γ value.

References

1) see M.M. Shapiro & R. Silberberg:
Space Science Reviews 36 51 (1983)

2) V.S. Berezinsky & V.L. Ginzburg:
Mon. Not. R. Astr. Soc. 194 3 (1981)

3) V.J. Stenger, DUMAND 80, Vol 1, 190 (1980)

4) T. Saito: in this workshop

5) V.S. Berezinsky: DUMAND 1979 Summer Workshop p245 (1979)
at Khabarovsk and Lake Baikal.

6) M. Kafatos; Ap. J. 236 99 (1980)

7) A. Strong, A.W. Wolfendale and J. Wdowczyk: Nature 24
109 (1973)

8) V.J. Stenger: HDC-7-83, to be published in Ap. J.

9) H. Lee and A. Bludman: UPR-02959T (7/27/84)